*Research supported by an institutional grant from the Alfred P. Sloan Foundation.

[1]G. Lachs, Phys. Rev. 138, B1012 (1965).
[2]H. Morawitz, Phys. Rev. 139, A1072 (1965).
[3]R. J. Glauber, in *The Physics of Quantum Electronics*, edited by P. L. Kelley, B. Lax, and P. E. Tannenwald (McGraw-Hill, New York, 1966), p. 788.
[4]P. J. Magill and R. P. Soni, Phys. Rev. Letters 16, 911 (1966).
[5]V. Korenman, Phys. Rev. 154, 1233 (1967).
[6]G. Lachs, J. Appl. Phys. 38, 3439 (1967).
[7]M. D. Aldridge, J. Appl. Phys. 40, 1720 (1969).
[8]E. Jakeman and E. R. Pike, J. Phys. A 2, 115 (1969).
[9]J. Peřina and R. Horák, J. Phys. A 2, 702 (1969).
[10]A. K. Jaiswal and C. L. Mehta, Phys. Rev. A 2, 168 (1970).
[11]G. Bédard, Phys. Rev. 161, 1304 (1967).
[12]C. D. Cantrell, Phys. Rev. A 1, 672 (1970).
[13]A. K. Jaiswal and C. L. Mehta (unpublished).
[14]R. Kubo, J. Phys. Soc. Japan 17, 1100 (1962).
[15]R. F. Chang, V. Korenman, C. O. Alley, and R. W. Detenbeck, Phys. Rev. 178, 612 (1969).
[16]C. L. Mehta, in *Lectures in Theoretical Physics*, edited by W. E. Brittin (Colorado U. P., Boulder, Colorado, 1965), Vol. VII, p. 345. See especially p. 398.
[17]R. J. Glauber, in *Quantum Optics and Electronics*, edited by C. DeWitt, A. Blandin, and C. Cohen-Tannoudji (Gordon and Breach, New York, 1965), p. 65. See especially Eq. (14.36).
[18]L. Mandel, J. Opt. Soc. Am. 51, 1342 (1961); L. Mandel and E. Wolf, Rev. Mod. Phys. 37, 231 (1965), Sec. 5.5.
[19]A. K. Jaiswal and C. L. Mehta, Phys. Rev. 186, 1355 (1969).

PHYSICAL REVIEW A VOLUME 3, NUMBER 2 FEBRUARY 1971

Zero-Field Mobility of an Excess Electron in Fluid Argon†

James A. Jahnke,* Lothar Meyer, and Stuart A. Rice
Department of Chemistry and James Franck Institute, The University of Chicago, Chicago, Illinois 60637
(Received 19 August 1970)

Drift velocities of electrons in fluid argon have been measured at temperatures from 90 to 160 °K and at pressures from 10 to 100 atm for applied electric fields in the range − 25 to − 200 V/cm. The electron drift velocity is found to be linear with respect to electric field strength only to − 100 V/cm at temperatures from 90 to 125 °K and to become increasingly nonlinear at temperatures greater than 125 °K. Mobilities can be obtained from these data by extrapolation to zero field; maxima are found in the zero-field mobilities as a function of density, in the region of 0.81 g/cm^3. Using the model proposed by Lekner for electron scattering by a system of fluctuating potentials and assuming that the scattering length for electrons in fluid argon approaches zero at some density, it is possible to obtain a semiempirical relation for the zero-field mobility as a function of density. Excellent agreement between calculated and observed mobilities is found in the high-density range studied 1.0–1.4 g/cm^3. At densities less than 1.0 g/cm^3, several qualitative aspects of the experimental data are accounted for by the theory, but quantitative agreement is lacking. It is possible that at these lower densities, gas-like scattering is of dominant importance.

I. INTRODUCTION

The injection of excess electrons into liquids provides a means of studying the electronic states of disordered systems. By adding an electron to a liquid, a conducting state becomes populated; to interpret the resultant electronic behavior it is necessary to develop physically realistic models correlating the electron-atom interactions with properties of the fluid. As might be expected, one of the most useful guides in such a development is provided by measurement of the electron drift velocity v_D (due to the application of an electric field E to the liquid). Now, the liquid systems which in principle are the simplest to understand are He, Ne, Ar, Kr, and Xe, primarily because of the spherical symmetry of the single-atom scattering potential, the absence of inelastic collisions, and the weak and short-range nature of the electron-atom interaction. This paper reports new measurements of the electron drift velocity in Ar and their interpretation.

In a dielectric liquid, such as liquid argon, where the resistivity is high (approximately 10^{19} Ω cm), the number of electrons that can be introduced into the liquid without producing space-charge effects is very small, on the order of 10^5–10^8 cm^{-3}.[1] The Coulomb energy between a pair of electrons is, then, less than the thermal energy k_BT (where k_B is the Boltzmann constant), and it becomes possible to measure directly the resistance to the electron motion arising from scattering of the electron by the fluid. The parameter of interest is the zero-field mobility, defined as $\mu_0 = \lim(v_D/E)$, as the

electric field strength approaches zero. The drift velocity is linear with respect to field strength in fluid argon only in a restricted range of fluid densities, and then only in fields generally less than -150 V/cm.[2,3] Much confusion has arisen in the literature because of the reporting of "apparent" mobility ($\tilde{\mu}$) measurements made in liquids at field strengths in excess of 1 kV/cm; in these fields the drift velocity is nonlinear with respect to the field.[4,5] Although additional information about electron-atom interactions may be deduced from apparent mobilities,[6–8] the saturation of the drift velocity at high-field strengths gives rise to phenomena difficult to interpret.[9]

Schnyders, Rice, and Meyer[3] were the first to study the low-field mobility of excess electrons over a range of densities in fluid argon. Among their observations were an anomalous rise in the apparent mobility near 115 °K on a 57-atm isobar in liquid argon, and a maximum in the apparent mobility at 180 °K on a 30-atm isobar in liquid krypton. This behavior has caused speculation on the possible existence of a Ramsauer-Townsend effect[10] for electron scattering in the liquid rare gases, although an alternative interpretation has been given by Lekner.[11,12] Because of the important consequences of the observations mentioned for any theory developed to describe excess electrons injected in rare gas liquids, it was decided to study the zero-field mobility of electrons in

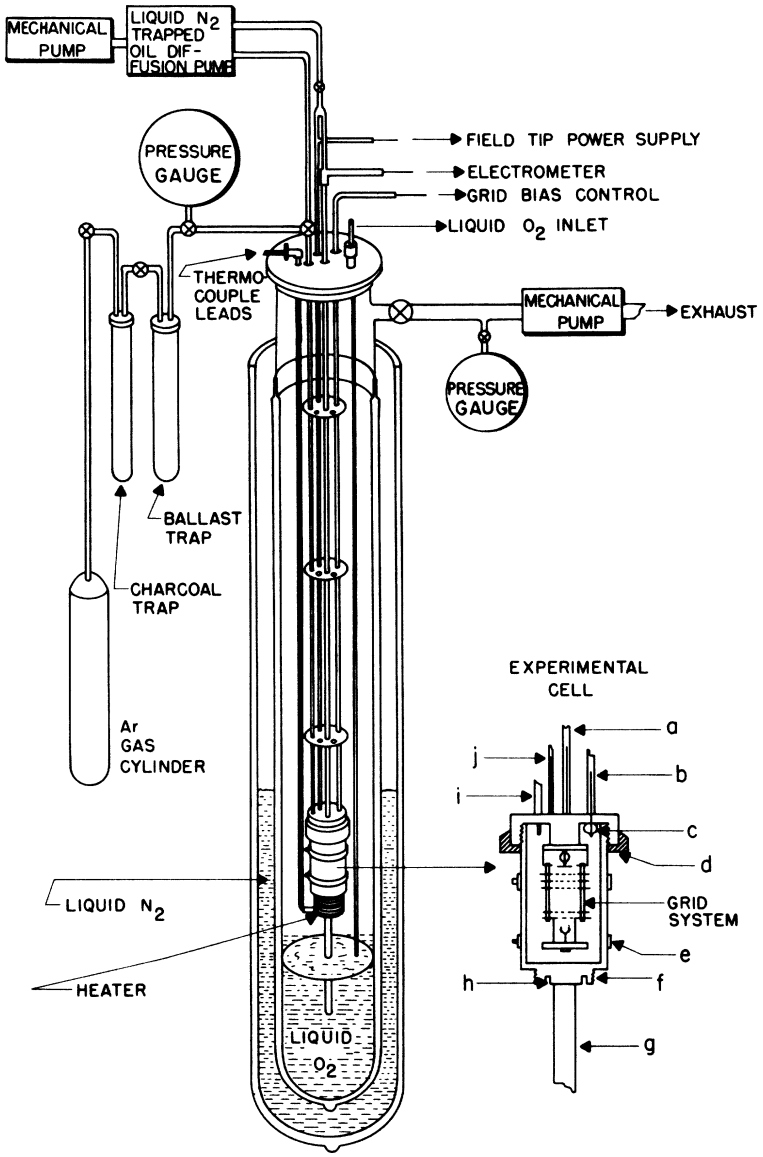

FIG. 1. Diagram of the cryostat, cell system, and external connections. Refer to Fig. 3 for a detailed electrical schematic. Identifications for the experimental cell are as follows: (a) evacuated electrometer lead; (b) evacuated high-voltage lead to field tip; (c) high-pressure kovar-glass seal; (d) tin-indium seal cup; (e) thermocouple ring; (f) screw-thread support for heater ring; (g) heat-leak rod; (h) thermocouple wells; (i) gas inlet tube; and (j) lead tubes for grids.

fluid argon over a range of densities extending from the triple point to the critical point.

II. EXPERIMENTAL DETAILS

The electron drift velocity was determined by a time-of-flight method used previously by Schnyders, Rice, and Meyer.[3] In the present experiments, a field-emission tip was used exclusively as a source of electrons. It was found that by properly preparing the tip and limiting the current through the tip, low-noise signals could be obtained over a wide range of densities in highly purified argon.

A. Argon Purification

Commercial tank argon of 99.995% purity was purified in three separate procedures. 100 liters of gas was first prepurified in a glass vacuum-purification system consisting of a mercury diffusion pump, a column of copper turnings heated to 350 °C, and two 2-liter tantalum getter bulbs.[13] A vacuum of 2×10^{-7} mm Hg was obtainable in the system with the copper column at 600 °C, the tantalum films being deposited on the walls of the bulbs under these conditions. Fresh tantalum films were deposited twice during the prepurification, the argon was then passed through the column and bulbs at a rate of 300 cm^3/min and collected in high-pressure stainless-steel storage cylinders by cryopumping.

Prior to each experimental run, the argon was further purified by passage through a trap of 45 g of activated cocoanut charcoal, the trap being immersed in a dry-ice–acetone mixture. The charcoal was degassed before each run by heating the trap to 600 °C and simultaneously pumping to a pressure of 1×10^{-6} mm Hg with a liquid-nitrogen–baffled oil diffusion pump for 2–3 h (see Fig. 1).

The third, and most important step of the purification procedure was to remove trace amounts of electron trapping impurities by an electrolytic method first developed by Schnyders.[2,3] In this method, the amount of gas to be used in the experimental run is liquified in the high-pressure experimental cell with a constant electric field of − 100 V/cm maintained across the cell. By producing an electric current in the system with the field-emission tip, electron trapping impurities can be electrolyzed out within 2–3 h. The magnitude of the current increases in this procedure from approximately 2×10^{-13} to 5×10^{-12} A, indicating the presence of an electron current in excess of that from the slower charged-particle species. Lekner[8] estimated that the impurity level should be less than 10 ppm if meaningful electron drift velocities are to be measured. By using sufficiently prepurified argon, impurity concentrations of less than 1 ppm may be obtained by the electrolytic method.[3]

B. Apparatus

The drift velocities were measured in an experimental system capable of containing liquid pressurized to 120 atm. Details of the pressurization system, cryostat, and experimental cell are shown in Fig. 1. Pressures were measured with a calibrated Heise gauge having a maximum error of 3 lb/in.^{2} Temperatures were controlled by balancing the heat input to a heating coil attached to the cell against a cold sink of liquid oxygen connected to the cell by means of a heat-leak rod. Seven copper-constantan thermocouples calibrated against a Natl. Bur. Std. platinum resistance thermometer[14] were used to monitor the temperature of the cell. Three thermocouples were placed in wells on the bottom of the cell, while four were placed along the length of the cell by means of copper rings. Heater input was regulated by means of a temperature controller sensitive to the null detector output of a thermocouple fixed to the bottom of the cell. It was possible to keep the cell temperature constant to within 0.1 °K by this method.

The grid system, as shown in Fig. 2, was connected to the base of the experimental cell and enclosed by a threaded copper cylinder made pressure tight by melting tin-indium solder in a trough surrounding the cylinder and its mating cap. Glass-kovar terminals[15] effectively withstood the high pressures of the system as electrical leads out of the cell. The grid system of the drift-velocity spectrometer as originally developed[16,17] consists of an ion or electron source, two sets of electrical shutters (grids *SA* and *BB'*), a main drift space between them, a current collector, and a Frisch grid used to prevent the alternating electric potential of the shutters from affecting the collector current. The modifications developed in the present experiments were in response to the

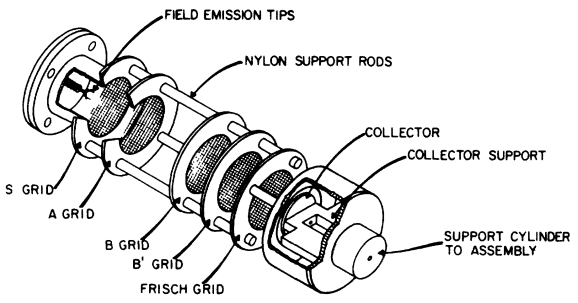

FIG. 2. Orthographic projection of the cell grid system.

use of a field-emission tip as an electron source. As shown in Fig. 2, the first grid consists of a gold-plated cylindrical shell surrounding two tungsten field-emission tips supported on a platinum-wire cross bar mounted onto a Teflon insulating disk. Several initial problems were incurred because of the large current (10^{-6} A) received by the cylindrical wall. Halpern and Gomer[13] found that currents greater than 10^{-7} A in liquid argon produce a pinpoint of purple light about the tip with consequent blunting of the tip. A current-limiting resistor of 10^{12} Ω (Fig. 3) controlled this grid current sufficiently to allow collector currents to 10^{-11} A to be obtained with an applied tip potential of between − 900 and − 2000 V. The field-emission tips provided low-noise collector currents over the range of densities covered in these experiments. It was found, however, that at low densities (< 0.7 g/cm^3) the rate of blunting would increase and the tips would eventually have to be replaced in order to reduce noise and the voltage necessary for electron discharge.

C. Experimental Method

The time of flight of electrons in liquid argon was measured over the main drift space AB of the spectrometer. When an electric square-wave potential is applied to grids S and B', the grid pairs SA and BB' act as electric shutters which open and close with the frequency of the applied square wave. The number of electrons, drifting under the influence of the applied electric field E, that will reach the collector will be a maximum whenever the time T_0 required for the electrons to drift the distance s_0 from A to B is equal to an integral number of periods ν^{-1} of the gating potential. The collector current will then be a periodic function of ν, the applied square-wave frequency. More detailed analyses of the operation of the drift-velocity spectrometer may be found elsewhere.[3,17,18]

The continuously scanned output from a Hewlett-Packard model 211A square-wave generator was split and amplified, the output frequencies being measured by a Hewlett-Packard model 5245L electronic counter. Applied grid potentials were derived from 300-V batteries, being subdivided by 10-turn Beckman Helipots. Electron collector currents were measured with a Cary model 31 vibrating-reed electrometer, and recorded on an X-Y recorder, whose X axis was coupled to the motor drive of the frequency generator (Fig. 3).

In performing a given experiment, the experimental cell and gas system would be pumped to a pressure of 1×10^{-6} mm Hg or less for a period of 12 h. The cell would then be flushed three times with gas which had passed through the charcoal purifier, and be evacuated after each flushing. After the third flushing, the cell would be pressurized

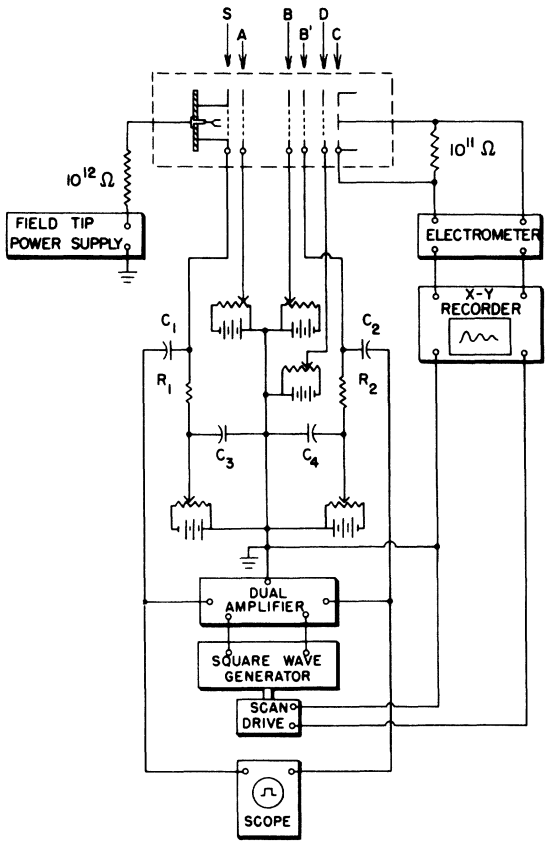

FIG. 3. Diagram of the grid system and the external circuits necessary for shutter control and current measurement. Dashed lines indicate the part of the grid system enclosed in the experimental cell. Values of the resistances and capacitances are $R_1 = R_2 = 1.5$ MΩ; $C_1 = C_2 = 4.0$ μF; $C_3 = C_4 = 2.02$ μF.

to about 5 atm, liquid nitrogen would be poured half way up the outer Dewar, and liquid oxygen added to the inner Dewar of the cryostat to cover the cell. Argon gas would then be liquified in the cell and pressurized to 100 atm. Grid voltages would be adjusted to produce a constant field of − 100 V/cm and the field-tip voltage set at − 2000 V. A transient burst of emission is seen on first application of the field-tip voltage,[13] but quickly dies down to a stable emission current. The collector current increases by an order of magnitude during the 2-h electrolysis period and attains a steady value of about 1.5×10^{-12} A. The temperature of the cell could then be raised to the desired value and the pressures varied to obtain drift-velocity data on an isotherm. Data were also taken along isobars, particularly at the higher temperatures (Fig. 4). At each experimental point (pressure and temperature dependent), drift-velocity measurements were taken at − 25, − 50, − 75, and − 100 V/cm,

except in some cases where the drift velocity was obviously linear with respect to field, and measurements were taken only at −75 and −100 V/cm. Several attempts were made to use cryogenic fluids, such as Freon-14, to control the temperature of the cell, but problems were incurred in electrolytically purifying the liquid argon at temperatures higher than 90 °K. Data taken with Freon-14 as a coolant, however, agreed well with those obtained by using the heat-leak method.

Figure 4 shows a temperature-pressure grid over which the data of this paper were taken. The data extend from densities of 1.41 g/cm^3 in the dense liquid, to 0.38 g/cm^3 in the supercritical region of the fluid.

III. EXPERIMENTAL RESULTS

A comparison of data obtained in these experiments with those of other workers is possible only in limited density ranges. Data obtained by Schnyders,[3] using a polonium-210 electron source, are shown with data obtained here, using a field-emission tip in Fig. 5. Agreement is within 10%, as it is with most of the other data overlapped by these experiments. The data of Halpern *et al.*[19] (with argon estimated as having an impurity level of $< 10^{-3}$ ppm), and of Miller, Howe, and Spear[7] were taken essentially at the vapor pressure of argon at 85 °K. Although no data were taken under these conditions here, data obtained on the vapor-pressure curve at higher temperatures were extrapolated to 85 °K to give a value for μ_0 of approximately 520 cm^2/V sec, to be compared to the value 475 cm^2/V sec of Miller *et al.*,[7] and of about 560 cm^2/V sec of Halpern *et al.*[19] Schnyders obtained a value of 470 cm^2/V sec at 85 °K and 6.0 atm. Figure 5 also shows a comparison of isobaric and isothermal experiments. The substantial agreement between them indicates that the pressure-temperature dependence of the mobility does not depend upon the method of varying these parameters.

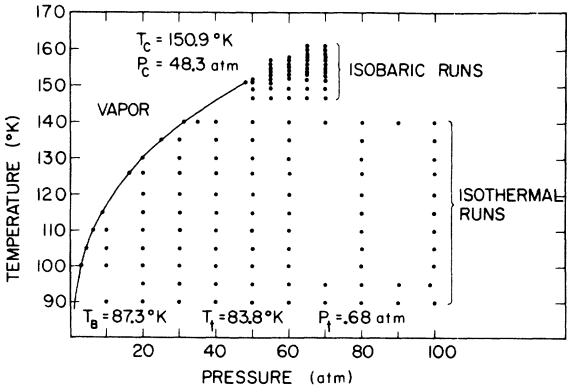

FIG. 4. Experimental data grid. Each point corresponds to a given temperature and pressure at which drift-velocity measurements were taken from −25 to −100 V/cm at 25-V intervals.

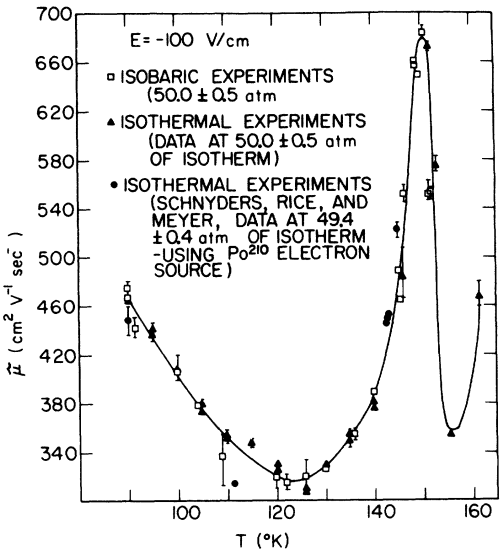

FIG. 5. Comparison of apparent mobilities at −100 V/cm on a 50-atm isobar in liquid argon. Data from the isothermal experiments were obtained by taking the value at 50 atm from plots of apparent mobility versus pressure at constant temperature. Refer to Ref. 3 for data obtained using a Po^{210} electron source. The figure shows the agreement between data using different sources and between data obtained through different thermodynamic routes.

Each drift-velocity measurement we report is the average of from 6 to 10 scans by the spectrometer, an equal number of scans being obtained by sweeping from lower to higher frequencies and from higher to lower frequencies. The precision estimates from these averages give a less than 2% deviation for drift velocities in the density range 1.4–1.1 g/cm^3 and a less than 4% deviation for drift velocities at densities lower than 1.1 g/cm^3. By repeating several experiments, particularly in the ranges of about 1.4 and of 0.8 g/cm^3, it was estimated that the drift velocities are accurate to within 5%, data obtained at higher densities being somewhat more accurate.

Figures 6–10 show the behavior of the electron-drift velocity with respect to applied electric field for five isobars. At temperatures from 90 to 120 °K (corresponding to densities greater than 1.0 g/cm^3) the drift velocities are linear to −100 V/cm and are not shown in these figures. The drift velocity becomes increasingly nonlinear for densities less than 1.0 g/cm^3 and has the greatest nonlinearity at densities corresponding to the maxima men-

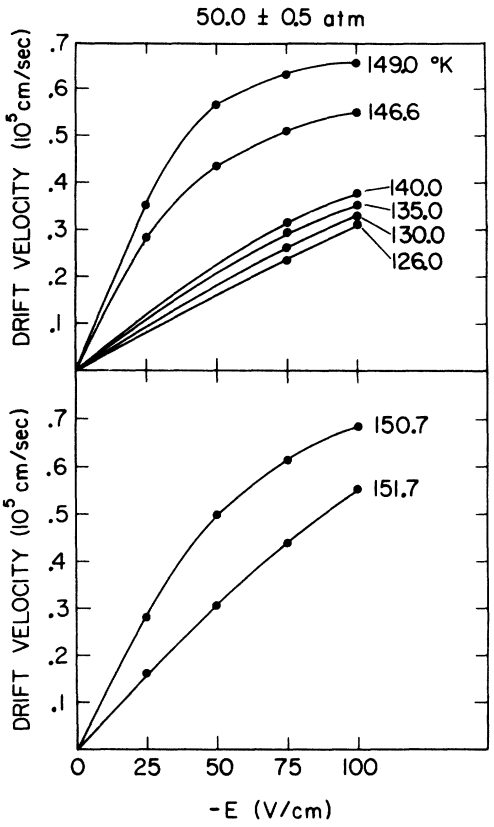

FIG. 6. Electron drift velocity versus electric field strength at 50 atm.

tioned earlier. Miller, Howe, and Spear have made the comment that "hot-electron" effects are observed when the velocity of sound in the liquid approaches the drift velocity.[7] Indeed, at a value of about 350–400 m/sec, where the drift velocity and sound velocities are almost equal, nonlinearity in the drift-velocity curves becomes pronounced. There is considerable crossing of drift-velocity curves near the maxima at about − 75 V/cm as shown in Figs. 8–10. These crossings are outside the error of the experiments and occur near the beginning of saturation of the drift-velocity curves.

The drift velocity again becomes linear on the low-density side of the maxima, and at densities less than the critical density 0.54 g/cm^3, the drift velocity even increases from the zero-field slope with increasing field.

Zero-field mobilities calculated from curves in Figs. 6–10 are included in Table I. The densities and isothermal compressibilities (χ_T) given in Table I were calculated from the parametrized equation of state for argon given by Gosman and coworkers.[20,21] Values of the sound velocity were obtained by interpolation and extrapolation from the works of Thoen, Vangeel, and Van Dael,[22] and of Radovskii.[23]

Zero-field mobilities are plotted versus number density in Fig. 11. The maxima are quite striking, occurring on different isobars at a common number density of approximately 0.012 Å^{-3} (0.81 g/cm^3). The maxima are followed on the high-density side by a minimum which is, however, much less pronounced. At densities lower than the critical density (0.008 Å^{-3} or 0.54 g/cm^3) the mobility again increases. This is to be expected since there should be a smooth approach to the higher mobilities characteristic of electrons in gaseous argon.[24,25]

The pressure dependence of the zero-field mobility is given in Figs. 12 and 13. From 90 to 126 °K, the mobility is linear with respect to pressure, the slopes of the isotherms slightly decreasing with increasing temperature. The pressure dependence is small over this range of temperatures, considering the greater dependence near the maximum. At 135 °K, the mobility shows no

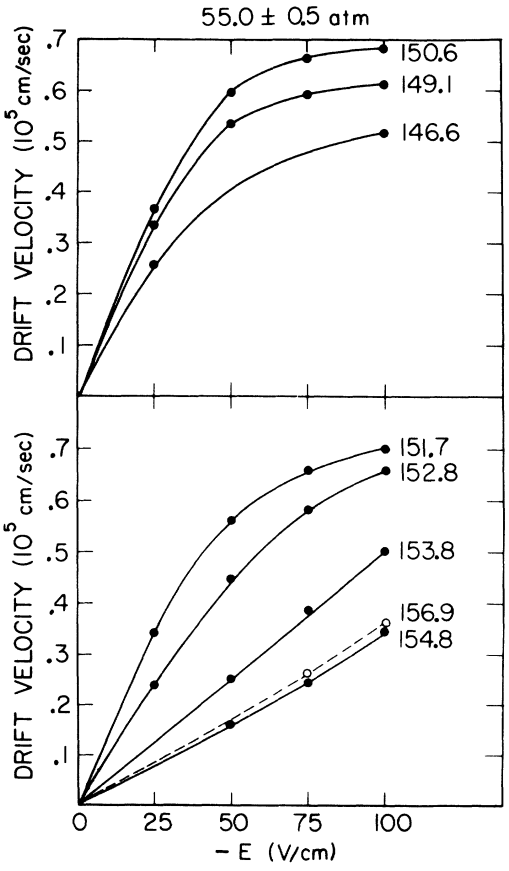

FIG. 7. Electron drift velocity versus electric field strength at 55 atm. Note the linear dependence at 153.8 °K.

TABLE I. Thermodynamic data and zero-field mobilities in argon.

P (atm)	T (°K)	ρ (g/cm^3)	n (Å^{-3})	χ_T (10^{-11} cm^2/dyn)	c (m/sec)	μ_0 (cm^2/V sec)
50.1	90.1	1.392	0.020 99	21.55	844.0	501
50.3	95.0	1.362	0.020 54	24.50	811.5	438
50.0	100.0	1.331	0.020 06	28.27	778.3	407
50.4	105.0	1.298	0.019 57	32.93	742.0	375
50.2	110.0	1.264	0.019 05	38.96	704.2	353
50.1	115.1	1.227	0.018 49	47.03	669.0	348
49.9	120.1	1.188	0.017 91	57.84	629.5	341
49.9	126.0	1.139	0.017 18	76.53	578.0	313
50.1	130.0	1.103	0.016 63	95.38	542.0	350
49.8	135.0	1.052	0.015 86	133.6	491.0	390
50.0	140.0	0.992	0.014 95	206.2	433.0	505
50.5	146.6	0.879	0.013 26	544.6	332.0	1140
49.9	149.0	0.811	0.012 23	1130	284.0	1407
50.2	150.7	0.732	0.011 03	3089	216.0	1119
50.9	151.7	0.654	0.009 87	9012	167.0	626
55.0	90.1	1.394	0.021 01	21.32	846.5	500
55.0	95.0	1.364	0.020 56	24.22	814.0	440
55.0	100.0	1.333	0.020 09	27.88	782.0	406
55.0	105.0	1.300	0.019 60	32.44	745.0	375
55.0	110.0	1.266	0.019 09	38.25	708.5	358
55.0	115.1	1.229	0.018 54	45.98	672.0	348
55.0	120.1	1.192	0.017 97	56.17	635.0	343
55.0	126.0	1.144	0.017 24	73.61	584.5	321
55.0	130.0	1.108	0.016 71	91.03	550.0	347
55.0	135.0	1.059	0.015 96	124.6	502.5	385
55.0	140.0	1.002	0.015 10	185.9	446.5	476
54.4	146.6	0.899	0.013 55	430.2	354.0	1032
54.4	149.1	0.842	0.012 70	734.5	314.0	1350
54.5	150.6	0.797	0.012 02	1171	276.0	1470
54.9	151.7	0.757	0.011 41	1799	253.0	1355
55.0	152.8	0.695	0.010 48	3610	218.0	966
54.8	153.8	0.587	0.008 84	9925	172.0	510
54.9	154.8	0.477	0.007 19	11006	181.0	332
55.0	155.9	0.410	0.006 18	8123	188.0	326
55.0	156.9	0.372	0.005 62	6521	192.5	358
60.2	90.1	1.395	0.021 03	21.09	849.0	501
60.0	95.0	1.366	0.020 59	23.94	807.2	442
60.3	100.0	1.335	0.020 12	27.48	785.0	410
60.2	105.0	1.302	0.019 63	31.91	749.0	377
60.1	110.0	1.268	0.019 12	37.52	712.0	360
59.9	115.1	1.232	0.018 58	44.97	677.0	350
59.5	120.1	1.195	0.018 01	54.79	640.0	343
59.9	126.0	1.148	0.017 30	71.03	591.0	333
59.6	130.0	1.113	0.016 78	87.33	557.0	356
59.9	135.0	1.065	0.016 06	117.3	512.0	382
60.0	140.0	1.011	0.015 24	169.6	458.5	455
59.7	146.6	0.917	0.013 83	346.6	379.0	892
60.1	149.2	0.870	0.013 12	517.1	341.0	1306
60.1	151.8	0.806	0.012 15	936.8	293.0	1608
59.5	152.8	0.767	0.011 57	1386	273.0	1413
60.0	153.7	0.737	0.011 11	1840	251.0	1367
60.1	154.8	0.682	0.010 29	3022	226.0	972
60.1	155.8	0.617	0.009 30	4871	181.0	703
60.2	156.8	0.548	0.008 25	6248	186.0	480
60.2	157.8	0.486	0.007 32	6374	192.0	366
65.0	90.1	1.397	0.021 06	20.88	851.3	503
65.0	95.0	1.367	0.020 61	23.66	820.0	444
65.0	100.0	1.336	0.020 15	27.13	788.0	411

TABLE I. (*Continued*)

P (atm)	T (°K)	ρ (g/cm^3)	n (Å^{-3})	χ_T (10^{-11} cm^2/dyn)	c (m/sec)	μ_0 (cm^2/V sec)
65.0	105.0	1.304	0.019 66	31.44	753.0	380
65.0	110.0	1.271	0.019 16	36.86	716.2	362
65.0	115.1	1.235	0.018 62	43.97	682.0	354
65.0	120.1	1.198	0.018 07	53.20	645.0	346
65.0	126.0	1.152	0.017 37	68.56	597.0	323
65.0	130.0	1.118	0.016 86	83.38	564.0	351
65.0	135.0	1.072	0.016 16	110.6	518.0	385
65.0	140.0	1.019	0.015 36	156.1	465.0	440
65.0	146.7	0.932	0.014 05	294.8	395.0	780
65.0	149.1	0.892	0.013 45	404.8	366.0	1030
65.0	151.7	0.839	0.012 66	630.2	328.0	1437
65.1	152.8	0.813	0.012 26	790.0	309.0	1583
65.1	153.7	0.788	0.011 88	991.0	295.0	1541
65.0	154.8	0.754	0.011 37	1333	272.0	1490
65.1	155.8	0.717	0.010 80	1828	252.0	1249
65.0	156.7	0.675	0.010 18	2512	234.0	982
65.1	157.8	0.622	0.009 38	3441	208.0	750
65.2	158.8	0.572	0.008 63	4131	191.0	612
65.1	159.8	0.522	0.007 86	4519	196.0	517
65.1	160.9	0.477	0.007 19	4495	201.0	483
70.4	90.1	1.398	0.021 08	20.66	853.6	506
70.0	95.0	1.369	0.020 64	23.39	823.0	445
70.0	100.0	1.338	0.020 17	26.78	791.0	413
70.0	105.0	1.306	0.019 69	30.96	758.0	382
70.0	110.0	1.273	0.019 19	36.21	720.0	364
70.0	115.1	1.238	0.018 66	43.05	688.0	357
70.0	120.1	1.202	0.018 12	51.84	650.0	343
70.0	126.0	1.156	0.017 43	66.31	604.0	324
70.0	130.0	1.123	0.016 92	80.08	571.0	353
70.0	135.0	1.077	0.016 24	104.8	525.0	385
70.3	140.0	1.027	0.015 49	144.2	480.0	406
70.1	146.6	0.946	0.014 27	253.7	412.0	732
70.1	149.1	0.909	0.013 70	336.0	382.0	957
70.1	151.7	0.864	0.013 02	480.6	351.0	1363
69.9	152.8	0.840	0.012 67	580.9	335.0	1551
70.2	153.8	0.820	0.012 36	683.7	321.0	1647
70.1	154.7	0.798	0.012 03	822.4	309.0	1733
70.1	155.8	0.768	0.011 58	1046	292.0	1657
70.2	156.8	0.739	0.011 14	1315	275.0	1522
70.1	157.8	0.703	0.010 61	1705	258.0	1380
70.1	158.9	0.662	0.009 97	2222	238.0	1145
70.1	159.9	0.621	0.009 36	2717	216.0	892

pressure dependence, and at temperatures greater than 135 °K, the mobility becomes increasingly nonlinear with respect to pressure, reflecting effects of the mobility maxima.

The temperature dependence of the mobility on the 55-atm isobar is shown in Fig. 14. On the scale of the mobility range, values of the mobility from 90 to 126 °K on other isobars show approximately the same temperature dependence. Figure 15 shows the shift of the temperature of the maximum for different isobars. The shift of the mobility maxima with increasing pressure is essentially a reflection of the fact that they occur at approximately the same density, as was shown in Fig. 11.

IV. THEORETICAL CONSIDERATIONS

The first theoretical description of low-field electron mobilities in liquid argon was given by Schnyders, Rice, and Meyer.[3] Their analysis, which was later placed on firmer theoretical ground by Cohen and Lekner,[26] led to predictions in qualitative agreement with experimental data obtained in the liquid region at densities from about 1.4 to 1.2 g/cm^3. The theory, however, failed to give any explanation for the rise in the

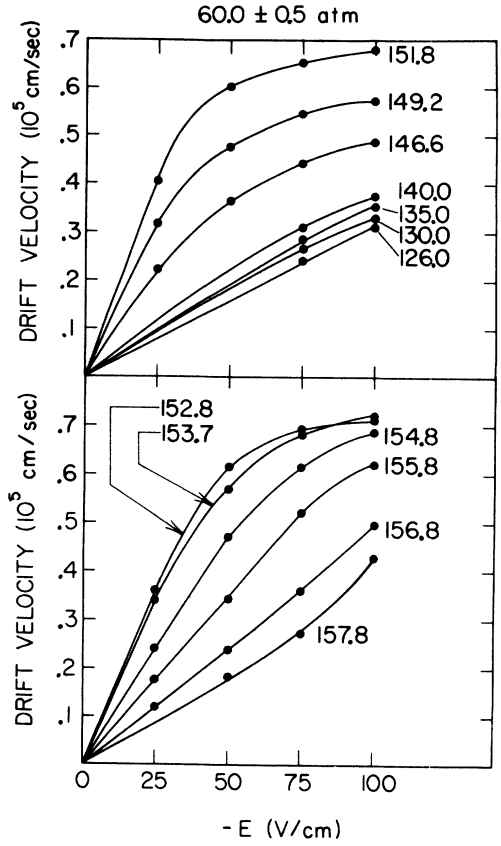

FIG. 8. Electron drift velocity versus electric field strength at 60 atm. Note the change of field dependence at 156.8 °K.

mobility at lower densities in the case of liquid argon and for the maximum observed in liquid krypton. The inadequacy in the theory was at that time felt to be due to the lack of knowledge of electron scattering cross sections in the liquid.[3] We will show that in order to calculate cross sections which account for the mobility maximum, it becomes necessary, as suggested by Lekner,[11,12] to consider fluctuations in the scattering potentials and the variation with density of the scattering length. In this section we shall describe some of the discrepancies between theory and experiment, and attempt to interpret the mobility maximum in fluid argon in terms of the zero scattering length model developed by Lekner.[11,12]

A. Mobility Equation

The mobility equation descriptive of electrons in liquid argon derived by Schnyders *et al.*[3] is based on a modified Boltzmann transport equation. By expanding the electron velocity distribution function in terms of the ratio of the velocity component in the electric field direction to the total velocity, and by use of the homogeneous linear differential equation (Chapman and Cowling[27])

$$[\epsilon + k_B T b(\epsilon)]\frac{df_0(\epsilon)}{d\epsilon} + \frac{\epsilon}{k_B T} f_0(\epsilon) = 0 , \tag{1}$$

they obtained the expression

$$f_0(\epsilon) = \exp\left[-\frac{1}{k_B T}\int_0^{\epsilon} \frac{\epsilon}{\epsilon + k_B T b(\epsilon)} d\epsilon \right] , \tag{2}$$

where $f_0(\epsilon)$ is the electron distribution function, ϵ is the electron energy, and $b(\epsilon)$ is an energy-dependent function involving scattering cross sections and the liquid structure. Cohen and Lekner,[26] by applying the Van Hove sum rules for the conservation of energy and momentum in the single-scatterer approximation, solved the Boltzmann equation to obtain the solution of Eq. (1) with

$$b(\epsilon) = \frac{1}{6}\frac{M}{m}\left(\frac{eE}{k_B T}\right)^2 \frac{1}{n^2 \sigma_0(\epsilon)\sigma_1(\epsilon)} , \tag{3}$$

where $\sigma_0(\epsilon)$ and $\sigma_1(\epsilon)$ are the total energy and momentum-transfer cross sections, respectively, and n is the argon number density (m is the electron mass, M the atomic mass). Schnyders's re-

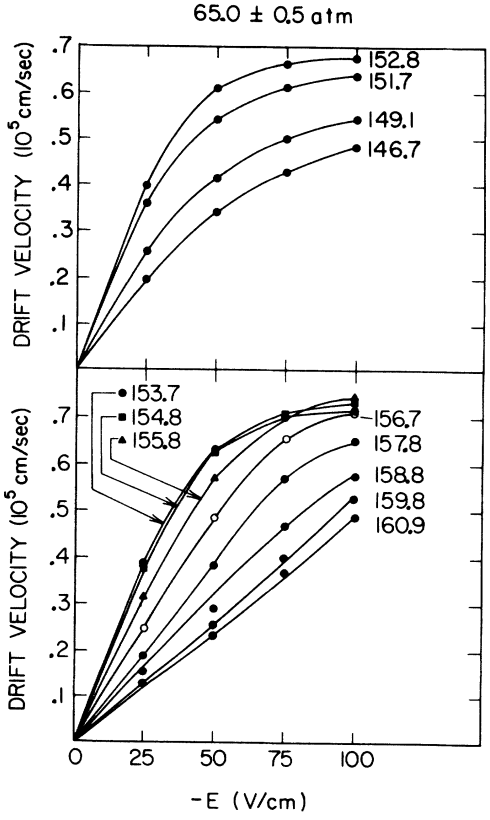

FIG. 9. Electron drift velocity versus electric field strength at 65 atm. Note crossings at temperatures near the maximum.

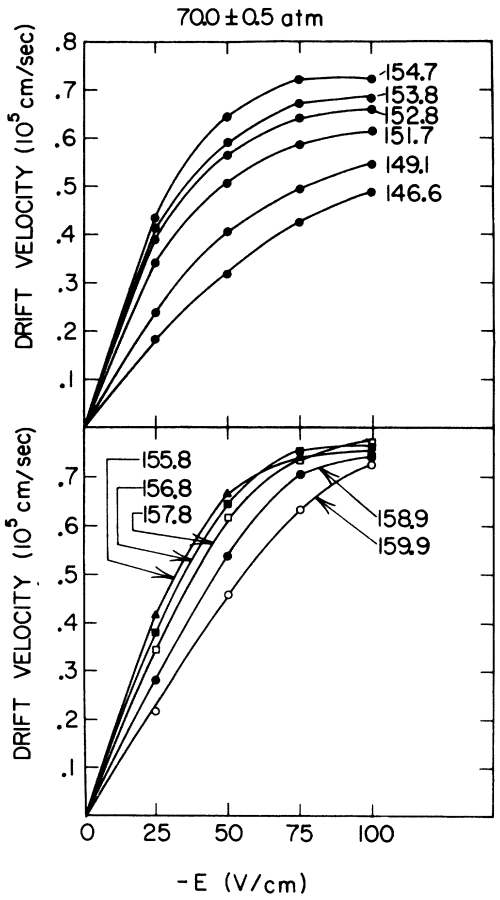

FIG. 10. Electron drift velocity versus electric field strength at 70 atm.

sult differs from this expression by the appearance of an energy-dependent momentum-transfer cross section $[Q_m^L(\epsilon)]^2$ in place of the product $\sigma_0(\epsilon)\sigma_1(\epsilon)$. The more detailed analysis by Lekner is correct in this case.

The drift velocity of an electron in a fluid can be expressed in terms of $f_0(\epsilon)$ and $f_1(\epsilon)$, the second term in the expansion of the velocity distribution, where

$$f_1(\epsilon) = \frac{eE}{n\sigma_1(\epsilon)} \frac{df_0(\epsilon)}{d\epsilon} , \tag{4}$$

$$v_D = \tfrac{1}{3}(2/m)^{1/2} \int_0^\infty \epsilon f_1(\epsilon)\, d\epsilon \Big/ \int_0^\infty \epsilon^{1/2} f_0(\epsilon)\, d\epsilon . \tag{5}$$

The integrated form of the electron-drift velocity ultimately depends on the form of $b(\epsilon)$. Schnyders *et al.*[3] performed calculations by using two assumed forms for $b(\epsilon)$ and by numerically integrating Eq. (5) using the energy-dependent $b(\epsilon)$. Unfortunately, at that time only gas phase scattering cross sections were available for argon; their theoretical results reflected this, particularly in giving an improper field dependence to the drift velocity (see Fig. 9 of Ref. 2). If one assumes that the field energy of the electron is greater than the thermal energy [i.e., $kTb(\epsilon) \gg \epsilon$ in Eq. (2)], one obtains the Druyvesteyn distribution for f_0. This distribution predicts an $E^{1/2}$ dependence in the drift velocity, a dependence which approximates the experimental data at intermediate field strengths, but is not observed in the lower range of field strengths studied here and by Schnyders. At low field strengths, the thermal energy becomes larger than the field energy and it is possible to neglect $b(\epsilon)$ in Eq. (2); one then obtains the Maxwellian distribution $f_0(\epsilon) = e^{-\epsilon/k_BT}$. When $f_0(\epsilon)$ is Maxwellian in form, the drift velocity is given by

$$v_D = \tfrac{2}{3}(2/\pi m k_B T)^{1/2} eE/n\langle\sigma\rangle , \tag{6}$$

where $\langle\sigma\rangle$ is the electron scattering cross section averaged over ϵ. In the limit of thermal energies it can be assumed that

$$\langle\sigma\rangle = 4\pi\tilde{a}^2 S(0) \approx 4\pi\tilde{a}^2 n k_B T \chi_T , \tag{7}$$

where $S(0)$ is the liquid structure factor for the electron wave vector $k = 0$, and where we define, for the moment, $\tilde{a}$ as an effective scattering length. This form implies that only s-wave scattering is important, a familiar assumption in the limit of zero energy. Using Eq. (7), we obtain in the limit of zero field

$$\mu_0 = \tfrac{1}{12} m(2/\pi m k_B T)^{3/2} e/n^2\tilde{a}^2\chi_T . \tag{8}$$

Equation (8), in essentially the form given, was obtained by both Schnyders *et al.*[3] and Lekner,[8] and is equivalent to the expression of Bardeen and Shockley[28] for the electron mobility in a nonpolar crystal. Using this expression, Schnyders obtained good (quantitative) agreement with experiment over the temperature range 84–115 °K at 7 atm. The rate of decrease of mobility with temperature was, however, observed to be less than that predicted by Eq. (8). This, as we will show, was due to the assumption that the scattering length $\tilde{a}$ is independent of temperature.

The total energy and momentum-transfer cross sections as a function of energy at 84 °K, the triple point of argon, were calculated by Lekner[8] and used in a numerical calculation of the electron drift velocity from Eq. (5). The theoretical field dependence of v_D was found to agree extremely well with experiment. After inclusion of multiple-scattering effects in the cross section and use of an effective electron mass, the zero-field mobility at 84 °K was predicted to be 540 cm^2/V sec. This value is only 5% away from that observed.

B. Effective Scattering Potential Model

The total energy-transfer cross section of Lek-

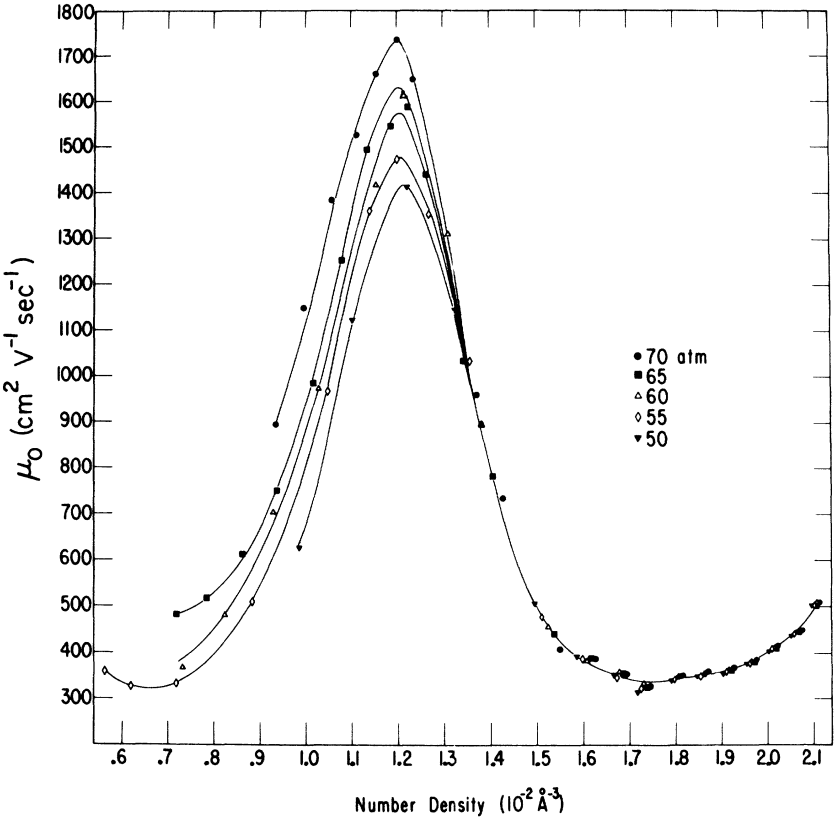

FIG. 11. Zero-field electron mobilities as a function of number density in fluid argon. This figure represents a summary of zero-field data obtained in these experiments.

ner[8] was obtained by using an effective electron scattering potential evaluated at 84 °K in the liquid. Because of screening effects in the liquid, it was found that the effective potential was not attractive enough to show a Ramsauer-Townsend effect at this temperature.

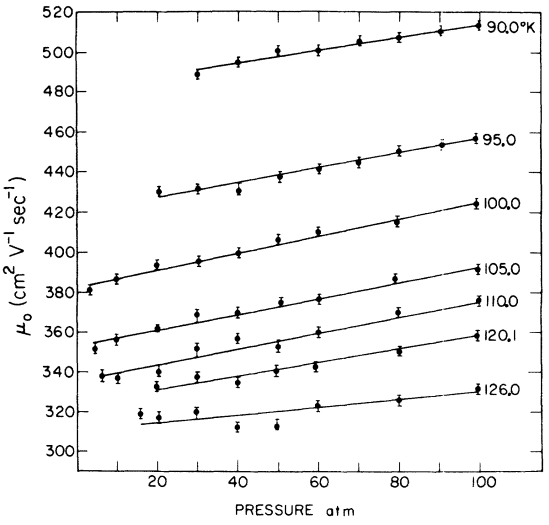

FIG. 12. Zero-field mobility of liquid argon as a function of pressure on isotherms from 90.0 to 126.0 °K.

Since, in the Ramsauer-Townsend effect, an attractive potential reduces the s-wave contribution to the scattering cross section to zero, the mag-

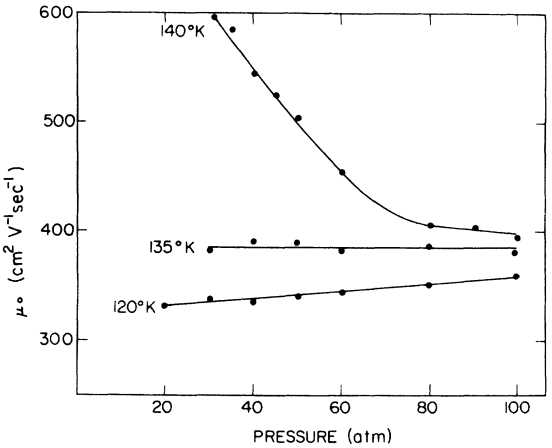

FIG. 13. Zero-field mobility of electrons in liquid argon as a function of pressure on isotherms from 120.0 to 140 °K. Note the onset of nonlinear behavior on the 140 °K isotherm. At temperatures greater than 140 °K, the mobility-versus-pressure curves reflect the maxima and undergo a change of slope at a temperature and pressure corresponding to the density at which the maximum occurs, 0.8 g/cm^3.

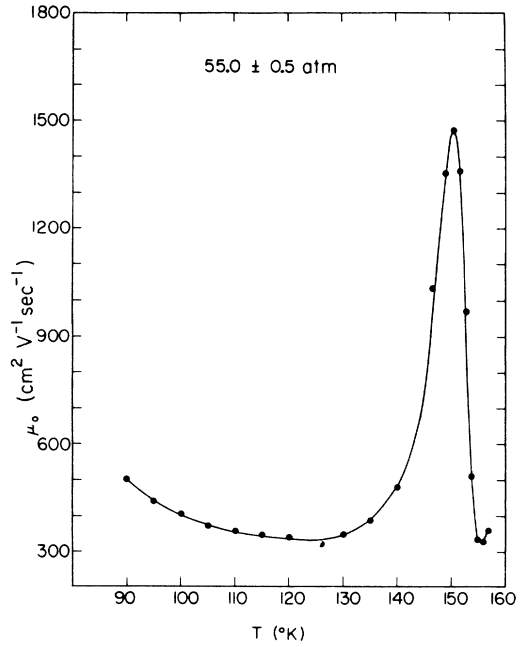

FIG. 14. Representative curve of electron zero-field mobility as a function of temperature. Note that the minimum on the low-temperature side of the maximum has a small depth compared to the height of the maximum. Also note the minimum on the high-temperature side of the maximum.

nitude of the total cross section will fall to low values over a particular energy range of the electron. Any such effect would become evident in the drift velocity through $b(\epsilon)$ [Eq. (3)] and $f_1(\epsilon)$ [Eq. (4)]. The drift velocity is approximately inversely proportional to the cross section and would, hence, increase with decreasing cross section. The formulation of the problem appears in the following question: Although it has been shown that the effective potential does not lead to a Ramsauer minimum at the triple point, how does the effective potential behave over a range of densities from the triple point, past the density at which the mobility maximum occurs and to the critical point? In an effort to answer this question, we have evaluated the screening functions, effective potentials, and total cross sections at six points in this density range.

The effective scattering potential includes the electron-atom polarization, exchange, and correlation potential (see Ref. 8):

$$U_\alpha(R) = -\tfrac{1}{2}\alpha e^2 f(R)/(R^2+R_\alpha^2)^2 , \tag{9}$$

where R_α is a parameter giving a measure of the strength of short-ranged correlation and exchange forces ($R_\alpha = 0.65$ Å).[29] Here, $f(R)$ is the local-field function, describing the screening of the polarization interaction of an electron and a particular atom by the dipoles induced in the surrounding atoms of the fluid.[8] The function $f(R)$ has the form

$$f(R) = 1 - \pi n\alpha \int_0^\infty \frac{ds}{s} g(s) \int_{|R-s|}^{R+s} \frac{dt}{t^2} f(t)\theta(R,s,t) , \tag{10}$$

$$\theta(R,s,t) = (3/2s^2)(s^2+t^2-R^2)(s^2+R^2-t^2) + (R^2+t^2-s^2) ,$$

where α is the atomic polarizability, $g(s)$ the pair-correlation function of the fluid, s the distance between two atoms, and R and t the distances of these two atoms from the electron. The expression for $f(R)$ is classical in the sense that the integral over t varies from $R = 0$, or, in other words, the electron penetrates the atom. Special note should be made of the fact that in the derivation of Eq. (10) fluctuations in the dipoles acting on the electron are assumed to be negligible. The local-field function was calculated at six densities by numerically iterating the linear integral equation for

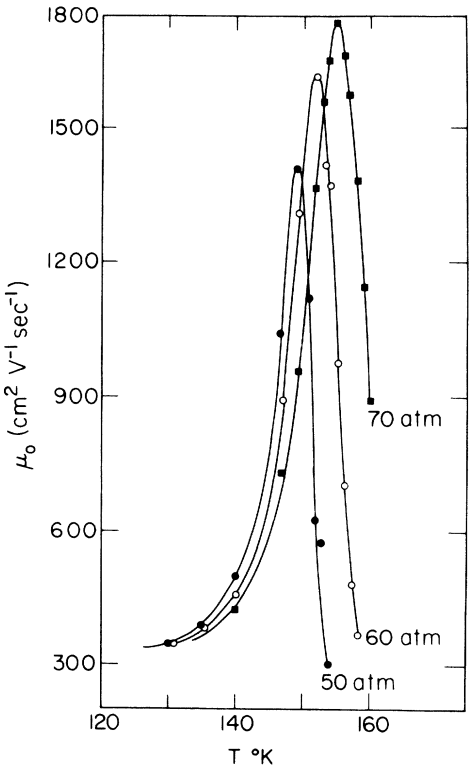

FIG. 15. Fluid argon zero-field mobility maxima as a function of temperature on three isobars.

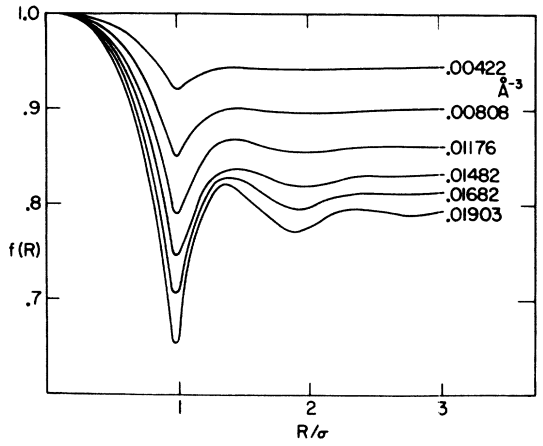

FIG. 16. The local-field function $f(R)$ due to a point charge calculated from experimental pair-correlation functions at different densities and a hard-core diameter $\sigma = 3.44$ Å.

$f(R)$ using the pair-correlation functions of Mikolaj and Pings[30] and of Smelser.[31] The results of these calculations are shown in Fig. 16. In the limit of the structureless fluid, where δ, the hard-core diameter of the atom, approaches zero, $g(s) = 1$ and $f(R)$ reduces to the Lorentz local-field function

$$f_L = (1 + \tfrac{8}{3}\pi n\alpha)^{-1}. \tag{11}$$

The value of $f(R)$ at large R approaches that of f_L, as can be seen from Fig. 16 and Table II.

The single-atom potential seen by the electron in the fluid then includes the Hartree screened Coulomb field of the nucleus U_H and U_α:

$$U_1(R) = U_H(R) + U_\alpha(R). \tag{12}$$

The effective potential for electron scattering is derived[8] by subtracting from the ensemble-average potential $\langle U(R)\rangle$ (which accounts for the overlapping of potential fields) a constant potential U_0, thus correcting for the fact that the electron only sees differences in the potential:

TABLE II. Effective potential parameters.

n (Å^{-3})	f_L	R_m (Å)	$-U_0$ (Ry)
0.019 03	0.794	2.20	0.121
0.016 82	0.813	2.25	0.109
0.014 82	0.832	2.27	0.099
0.011 76	0.862	2.32	0.087
0.008 08	0.901	2.40	0.070
0.004 22	0.945	2.55	0.047

$$\langle U(R)\rangle = U_1(R) + (2\pi m/R)\int_0^\infty ds\, sg(s)\int_{|R-s|}^{R+s} dt\, tU_1(t), \tag{13}$$

$$U_{eff}(R) = \langle U(R)\rangle - U_0, \quad R < R_m$$
$$= 0, \quad R > R_m \tag{14}$$

where R_m and U_0 are defined by

$$\left(\frac{\partial\langle U(R)\rangle}{\partial R}\right)_{R_m} = 0, \quad \langle U(R_m)\rangle = U_0.$$

The ensemble-average atomic potentials are shown in Fig. 17. Values for R_m and U_0 are given in Table II.

Cross sections were calculated by the method of partial waves at energies to 4 eV for each of the densities given in Table II. The use of these cross sections in the full numerical calculation of Eq. (5) gives a steadily decreasing zero-field mobility as a function of density with no maximum appearing over the range of densities studied. In fact, if one takes the gas scattering cross section of Frost and Phelps,[32] containing the Ramsauer minimum, and calculates a mobility at the density of the maximum, a value is obtained which differs from the experimental result by two orders of magnitude.

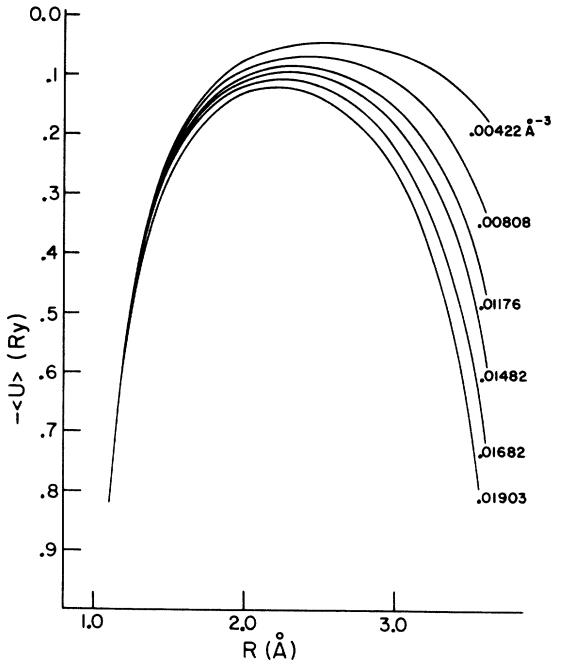

FIG. 17. The ensemble-average atomic potential for electron scattering in fluid argon over a range of densities

It should be noted that if at the low electric fields of these experiments one can approximate the electron distribution function as being Maxwellian, the average electron energy will equal $\frac{3}{2}k_BT$ and does not vary significantly on the scale over which changes in the cross section occur.

It is therefore felt that a Ramsauer-Townsend effect does not explain the behavior of electrons in fluid argon in a range of densities extending from the triple point to the critical point.

C. Zero Scattering Length Model

In his calculation of the electron scattering cross section for argon at the triple point, Lekner[8] found the scattering length in the liquid at this density to be positive and equal to $+0.76$ Å. Since the scattering length in the gas is negative, having a value of -0.87 Å at a density of about 0.05×10^{-2} Å^{-3},[33] he reasoned that somewhere in the density range of fluid argon the scattering length passes through the value zero. If this does occur, the electron mobility would then increase indefinitely at some density [Eq. (8)], its magnitude limited only by fluctuations in the scattering length. In an effort to explain the mobility maxima in rare-gas liquids, it therefore seemed reasonable[11] to express the scattering length as a sum of the average scattering length $\langle a\rangle$ and a fluctuation term Δa:

$$a=\langle a\rangle+\Delta a,\quad \langle a^2\rangle=\langle a\rangle^2+\langle\Delta a^2\rangle\,. \tag{15}$$

At the maximum, where the average scattering length $\langle a\rangle$ is presumed to be zero, $\langle a^2\rangle$ is nonzero and equal to $\langle\Delta a^2\rangle$.

Using the scattering law for a fluid of identical scatterers with a generalized correlation function (the correlations being between atomic positions and between scattering amplitudes), Lekner[12] showed that inclusion of the effect of fluctuations in the scattering length leads to the following relation for the total cross section:

$$\langle\sigma\rangle=4\pi(\langle\Delta a^2\rangle+\langle a\rangle^2 nk_BT\chi_T)\,. \tag{16}$$

The square of the effective scattering length defined in Eq. (7) is then equivalent to the expression in the parentheses except for the term $\langle\Delta a^2\rangle$, accounting for uncorrelated fluctuations. If $\langle\Delta a^2\rangle$ could be calculated, an estimate of the magnitude of the zero-field mobility at the maximum could be obtained from Eq. (6), since $\langle a\rangle$ would be equal to zero at that point. A knowledge of both $\langle\Delta a^2\rangle$ and $\langle a\rangle^2$ would give an expression for the mobility over a range of fluid densities.

An approximate calculation of $\langle\Delta a^2\rangle$ was performed, again by Lekner,[11] in terms of fluctuations caused in the effective atomic scattering potential by fluctuations in the positions of molecules in the liquid. These fluctuations are averaged over the possible directions of molecular displacement to obtain

$$\langle\Delta U^2\rangle=\tfrac{1}{3}\langle\Delta R^2\rangle 4\pi n\int_0^\infty dR\,R^2 g(R)(dU/dR)^2\,, \tag{17}$$

where R in this case is the distance between two atoms, $g(R)$ is the pair-correlation function, and $\langle\Delta R^2\rangle$ the mean-square molecular displacement. Fluctuations in the scattering length are related to fluctuations in the scattering potential in the Born approximation:

$$\Delta a=(2m/\hbar^2)\int_0^\infty dR\,R^2\Delta U\,. \tag{18}$$

To calculate Δa, Lekner assumed that U can be replaced by a constant over the range zero to R_s (where R_s is the Wigner-Seitz radius), its value equal to that at the origin. Then $\langle\Delta a^2\rangle$ becomes equal to

$$\langle\Delta a^2\rangle=(m/2\pi n\hbar^2)^2\langle\Delta U^2\rangle\,, \tag{19}$$

and the average total cross section at the maximum is

$$\langle\sigma\rangle=4\pi\langle\Delta a^2\rangle=4\pi(m/2\pi n\hbar^2)^2\langle\Delta U^2\rangle\,. \tag{20}$$

To calculate the mobility, Lekner made several severe approximations in the subsequent evaluation of $\langle\Delta U^2\rangle$. He assumed that (a) the mean-square displacement can be estimated from an Einstein model of atomic motions, which gives

$$\langle\Delta R^2\rangle=\tfrac{1}{3}R_s^2k_BT/Mc^2\,,$$

where c is the velocity of sound in the fluid; (b) $g(R)$ is accurately approximated by the pair-correlation function of a hard-sphere fluid with hard-sphere diameter δ; and (c) the effective atomic scattering potential U can be approximated by the Lorentz limit, Eq. (11). Using these assumptions in Eqs. (17) and (19) then gives

$$\langle\Delta a^2\rangle\approx\frac{4}{63}\frac{k_BT}{Mc^2}\frac{1}{\pi n\delta^3}\left(\frac{R_s}{\delta}\right)^2\left(\frac{\alpha f_L}{a_0\delta}\right)^2\,. \tag{21}$$

From Eq. (6) the zero-field mobility at the maximum becomes

$$\mu_0^{\max}\approx\left[\frac{63eM\delta^7}{6}\left(\frac{2\pi}{m}\right)^{1/2}\left(\frac{a_0}{R_s\alpha f_L}\right)^2\right]\frac{c^2}{(k_BT)^{3/2}}\,, \tag{22}$$

where a_0 is the Bohr radius. As observed by Lekner,[11] if one assumes the maxima to appear at an approximately constant density (f_L and R_s being

density dependent), the mobility at the maximum will be proportional to $c^2T^{-3/2}$. Calculations were performed using this model and the results were compared with the experimental data from Table I (see Fig. 19). The experimental value of 0.012 Å^{-3} for the density at the mobility maximum (n_{max}) was substituted in the theoretical calculation. The values of the sound velocities used in the calculations were obtained by interpolating and extrapolating the data of Thoen *et al.*[23] and of Radovskii.[24] The temperature dependence of the sound velocity at n_{max} on given isobars was linear to within 2%.

Figure 18 shows that there is extremely good agreement between the slopes of the experimental data and theoretical calculations. The error in the experimental data tended to be larger at densities near n_{max} than in other density ranges, the values of μ_0^{max} (expt) being average values with a maximum error of about 5%. With this consideration in mind, it can be said that experiment confirms the theoretically predicted $c^2T^{-3/2}$ dependence of μ_0^{max}. On the other hand, the magnitude of the theoretical zero-field mobilities are about 50% higher than the experimental mobilities. This is perhaps not surprising considering the many assumptions made in the evaluation of $\langle \Delta a^2 \rangle$, but it also may be possible that the magnitude of the mobility at densities near and less than n_{max} is decreased by some process not considered in the present theoretical model. This point will be discussed later. The closer agreement between theory and experiment obtained for μ_0^{max} in liquid krypton[11] (10%) is somewhat misleading because of the greater uncertainty in μ_0^{max} (expt) arising from a rather severe extrapolation of the apparent mobility data to zero field.

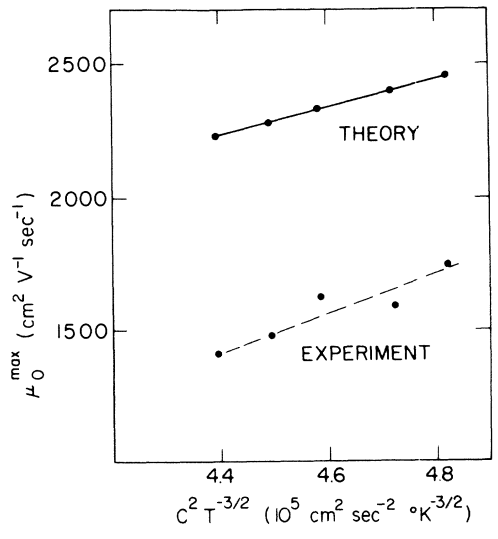

FIG. 18. Zero-field mobility magnitudes at the maxima as a function of $c^2T^{-3/2}$. The figure shows the correspondence between the experimental data and calculations from the zero scattering length model.

The zero scattering length model was further extended by Lekner[12] to predict a Lorentzian line shape for the mobility maximum. Taking the first term in a Taylor's series expansion of $\langle a \rangle$ near n_{max}, he obtained

$$\langle a \rangle = \gamma(n - n_{max}), \tag{23}$$

where $\gamma = (d\langle a \rangle/dn)_{n_{max}}$. Substituting Eq. (23) into (16) gives

$$\langle \sigma \rangle \simeq 4\pi[\langle \Delta a^2 \rangle + nk_B T\chi_T \gamma^2 (n - n_{max})^2], \tag{24}$$

$$\mu_0 \simeq \frac{2}{3}\left(\frac{2}{\pi mkT}\right)^{1/2} \frac{e}{4\pi n[\langle \Delta a^2 \rangle + nk_B T\chi_T \gamma^2 (n - n_{max})^2]}. \tag{25}$$

With $\langle a \rangle = 0$ at n_{max}, the ratio $\mu_0(n)/\mu_0(n_{max})$ obtained from Eq. (25) is

$$\frac{\mu_0(n)}{\mu_0(n_{max})} \simeq \frac{\langle \Delta a^2 \rangle_{max}}{\langle \Delta a^2 \rangle + nk_B T\chi_T \gamma^2 (n - n_{max})^2}, \tag{26}$$

with $\langle \Delta a^2 \rangle_{max}$ the mean-square fluctuation in the scattering length at the maximum.

The parameter γ was calculated using two methods. In the first method, the experimental zero-field mobilities for the isobars from 50 to 70 atm were substituted into Eq. (8) to obtain values of the effective scattering length $\tilde{a}$. The absolute values of $\tilde{a}$ were then plotted as a function of number density (see Fig. 19). If one assumes that $\langle \Delta a^2 \rangle$ is small compared to the second term in the brackets of Eq. (25), then $\tilde{a}$ will approximate $\langle a \rangle$. We assume that this condition is met on the linear portion of the curve of Fig. 19 from number densities of 0.0210 Å–0.0135 Å^{-3}. A particularly noteworthy observation from this curve is that the linear portion, on extrapolation, intercepts the density axis at the value of n_{max}. The absolute values of $\tilde{a}$ then increase at densities lower than n_{max}. This is precisely the behavior that one would expect from the zero scattering length model. A value for $\gamma = (d\langle a \rangle/dn)_{n_{max}}$ of 69.2 Å^4 was obtained from the slope of the linear portion. Calculations of $\langle \Delta a^2 \rangle$ using Eq. (21) and of the second term in the brackets of Eq. (25) using a value of $\gamma = 65.0$ Å^4 (see Table III) show that the condition on $\tilde{a}$ is met. For densities less than 0.014 Å^{-3}, these two terms become equivalent in magnitude and the interpretation of $\tilde{a}$ as a scattering length becomes somewhat dubious. It should be noted that this method of calculation of γ is dependent only on the assumption that $\langle \Delta a^2 \rangle$ is small and proceeds directly from the mobility Eq. (8).

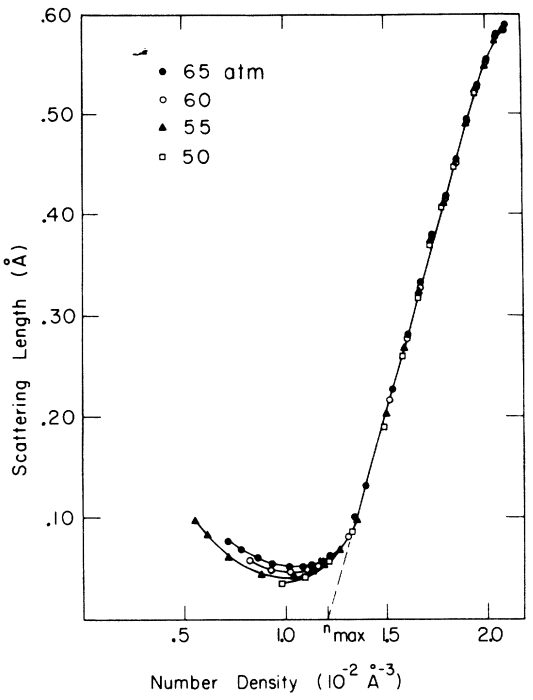

FIG. 19. Absolute values of the scattering length as a function of number density in fluid argon. Scattering lengths were obtained from the experimental data and the Lorentz formula for electron mobilities. Note the intercept of the curve at n_{max}, the density at which the maxima in Fig. 11 occur.

A more direct, but essentially equivalent, method of obtaining γ is to use Eqs. (26) and (21) with the experimental zero-field mobilities. If $\langle \Delta a^2 \rangle$ is small, the terms $\mu_0(n_{max})$ and $\langle \Delta a^2 \rangle_{max}$ get lumped in with the evaluation and the method becomes similar to the one above. A value for γ of 63.4 Å^4 was obtained by using 50 experimental mobilities over the range of densities cited above. This method does, however, give one an estimate of the validity of Eq. (26) in the region where fluctuations in the scattering length become important. At densities lower than 0.0140 Å^{-3}, values of γ deviate from the value that one would expect from an extrapolation of the curve of Fig. 19 to n_{max}. Furthermore, at densities lower than n_{max}, γ cannot be calculated since the estimates of $\langle \Delta a^2 \rangle$ from Eq. (21) make γ^2 negative. This is perhaps to be expected from the results of the calculation of μ_0^{max} from Eq. (21) previously cited.

Using a weighted value of $\gamma = 65.0$ Å^4, empirical zero-field mobilities were calculated from Eq. (25) for five isobars. As can be seen from Table III and Fig. 20, there is both qualitative and (essentially) quantitative agreement between theory and experiment in the range of densities from 0.021 to 0.040 Å^{-3}. The isothermal behavior of the zero-field mobility is well accounted for in this density region, the slopes of the theoretical isotherms being practically identical to the experimental isotherms. At densities in the region of 0.015 Å^{-3}, where the slope changes sign and the

TABLE III. Theoretical calculation of μ_0 at 55 atm with $\gamma = 65.0$ from Eq. (25). Values of γ are calculated from Eq. (26). Values of $\langle \Delta a^2 \rangle$ are from Eq. (21).

T (°K)	n (Å^{-3})	γ (Å^4)	$\langle \Delta a^2 \rangle$ (Å^2)	$nkT\chi_T\gamma^2(n-n_m)^2$ (Å^2)	$\mu_0^{theoret}$ $\left(\frac{cm^2}{V\ sec}\right)$	μ_0^{expt} $\left(\frac{cm^2}{V\ sec}\right)$
90.1	0.021 01	61.1	0.0001	0.0186	507.7	500
95.0	0.020 56	63.3	0.0002	0.0197	477.3	440
100.0	0.020 09	64.1	0.0002	0.0208	451.1	406
105.0	0.019 60	65.1	0.0002	0.0218	429.4	375
110.0	0.019 09	65.2	0.0003	0.0228	412.1	358
115.1	0.018 54	64.8	0.0003	0.0236	399.1	348
120.1	0.017 97	64.4	0.0004	0.0242	391.6	343
126.0	0.017 24	66.0	0.0006	0.0245	391.1	321
130.0	0.016 71	63.5	0.0007	0.0243	398.5	347
135.0	0.015 96	61.2	0.0010	0.0232	423.4	385
140.0	0.015 10	57.5	0.0014	0.0205	486.5	476
146.6	0.013 55	50.0	0.0029	0.0102	880.1	1032
149.1	0.012 70	53.5	0.0043	0.0027	1745.0	1350
150.6	0.012 02	•••	0.0062	0.0001	2031.7	1470
151.7	0.011 41	•••	0.0082	0.0089	788.3	1355
152.8	0.010 48	•••	0.0132	0.0897	142.6	966
153.8	0.008 84	•••	0.0294	0.8420	19.9	510
154.8	0.007 19	•••	0.0394	1.733	12.0	332
155.9	0.006 18	•••	0.0485	1.607	14.9	326
156.9	0.005 62	•••	0.0554	1.415	18.4	358

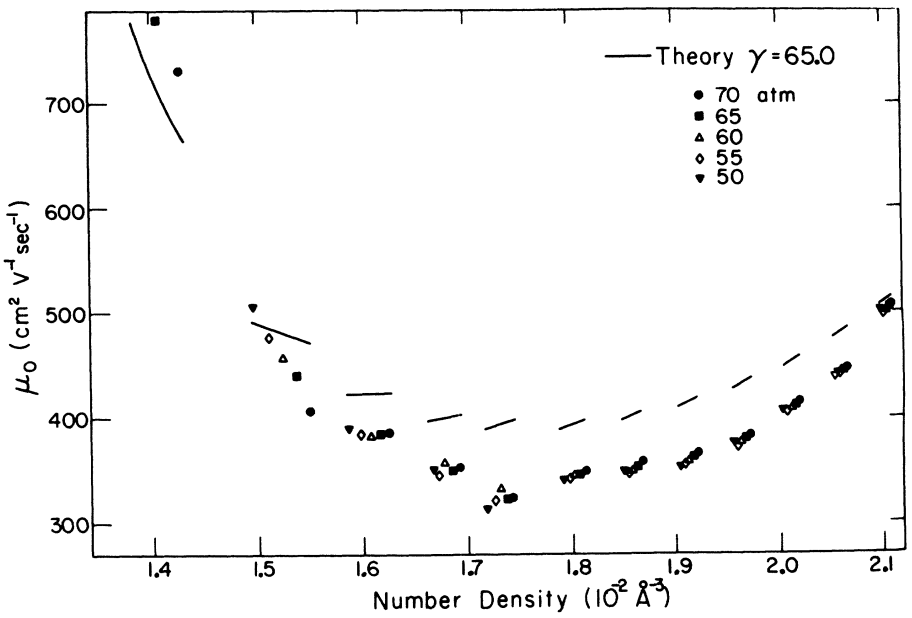

FIG. 20. Comparison of experimental and theoretical zero-field mobilities at densities greater than 0.014 Å^{-3}.

mobility becomes nonlinear with respect to pressure (see Fig. 13), even the qualitative agreement between theory and experiment is poor. Because of the empirical nature of the calculation of the parameter γ and the fact that $\langle \Delta a^2 \rangle$ is small in the high-density region, the theoretical mobility values agree to within 10 to 15% of the experimental values. Under these conditions, corrections for multiple scattering and an effective electron mass are included in the determination of γ, with the further assumption that they are density independent. The quantitative discrepancies which are observed in this high-density region may be indicative as to the validity of this assumption.

Table III gives theoretical values for zero-field mobilities calculated near the maximum and at lower densities for the 55-atm iosbar. Only poor quantitative agreement is obtained in this density range, with the theoretical mobility values near the maximum being too high, and near the critical point being an order of magnitude too low. Calculations on other isobars show that the theoretical isobaric curves will be nested as in Fig. 11 (i.e., mobility values decrease with decreasing pressure at a given density), although the theoretical calculations give a much smaller pressure dependence than is observed.

In an attempt to interpret the field dependence of the electron drift velocity, cross sections calculated from Eq. (24) using $\gamma = 65.0$ Å^4 were used in the evaluation of the electron distribution function $f_0(\epsilon)$ of Eq. (2). Drift velocities were calculated numerically from Eq. (5) for the 55-atm isobar. The results are shown in Fig. 21 and are to be compared with the experimental curves in Fig. 7. There is again good agreement between theory and experiment at the higher densities. At these densities, the theoretical drift velocity is nearly linear with respect to field, in accord with experiment, but at lower densities corresponding to temperatures greater than 140.0 °K, the $b(\epsilon)$

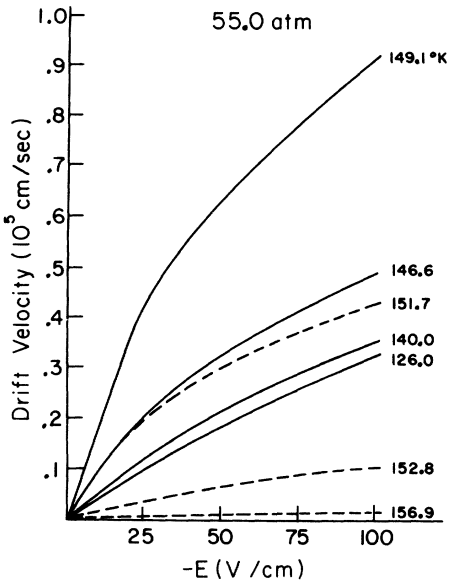

FIG. 21. Theoretical electron drift velocities as a function of electric field strength at 55 atm. The dashed lines distinguish curves on the low-density side of the maximum.

term in Eq. (2) becomes important and the drift velocity shows nonlinear behavior at very low fields. On the low-density side of the maximum, the field dependence is again linear, but there is an order of magnitude difference between theory and experiment as is expected from the equivalent mobility values given in Table III.

It can be seen, therefore, from calculations of drift velocities, zero-field mobilities, and magnitudes of the mobility maxima, that the zero scattering length model adequately explains the behavior of an excess electron in liquid argon at densities greater than 0.014 $Å^{-3}$, but becomes inadequate at lower densities. The discrepancies at low densities are basically quantitative, but also to some extent, qualitative. The theory does show that a maximum occurs in the mobility curve, as is obvious from the form of Eq. (25), but the theoretical mobility magnitudes at the maximum are 50% too high. The theoretical isobaric mobility curves nest about n_{max} as is found experimentally, but the theoretical mobilities fall too fast as a function of density on the low-density side of the maximum, and the nesting is not as distinct as is experimentally observed. Near the critical density, the theoretical mobilities are an order of magnitude too low, although they do begin to increase with decreasing density at $n = 0.007$ $Å^{-3}$ as is found experimentally. It should be noted here that isothermal compressibilities in this region, calculated from the parametrized equation of state of Gosman *et al.*[20,21] may be somewhat in error due to the behavior of the pressure differential at low densities.

V. DISCUSSION

In Sec. IV we have attempted to interpret our experimental results in terms of the present available theoretical models. The mean field theory of electron mobility in liquids accurately describes the behavior of an excess electron at the triple point.[8] The extension of the theory to lower densities requires an examination of the density dependence of the electron scattering cross section and the effect of fluctuations in the liquid on the form of the cross section. The effective scattering potential model does not alone provide an interpretation of the mobility maximum observed in fluid argon, but assuming that the scattering length, which is positive in the liquid and negative in the gas, goes through zero at some density and with the inclusion of a fluctuation term in the cross section, a greater understanding of the excess electron behavior has been obtained. The zero scattering length model gives both a qualitative and quantitative description of this behavior in a limited density range when a semiempirical relation for the mobility is employed. This relation, however, becomes inaccurate at densities lower than 0.014 $Å^{-3}$.

There are at present three possible explanations for the theoretical discrepancies: (i) The assumptions made in the estimations of $\langle \Delta a^2 \rangle$ are too severe to warrant the validity of Eq. (21) at low densities. (ii) Fluctuations in the liquid effect the mobility in some manner not accounted for by the zero scattering length model. (iii) Incipient electron localization influences the mobility on the low-density side of the maximum.

Better approximations to $\langle \Delta a^2 \rangle$ may be made by avoiding the limiting assumptions in the functions $f(R)$ and $g(s)$, but it is noted that these assumptions become more valid at lower densities. The estimates for the mean-square displacement used in Eq. (21) do, however, become invalid at these lower densities and it is probably in this direction that improvements in $\langle \Delta a^2 \rangle$ could be made. The nature of electron localization-delocalization in fluid argon is not well understood at present, but at densities near the critical density effects consistent with a model of gaslike scattering are being observed. Specifically, the drift velocity at these densities displays a concave-upward slope with respect to field, and the mobility at constant density increases markedly with increasing temperature.

The successes of the theory in interpreting the behavior of the excess electron in argon over the fluid density range are indeed encouraging. Further work on the theoretical interpretation of the low-density behavior and on the zero-field mobility measurements in other rare-gas liquids, such as neon and krypton, would contribute much to the understanding of the properties of excess electrons in disordered systems.

---

†Research supported in part by the National Science Foundation, under Grant No. GP8375, the Directorate of Chemical Sciences, AFOSR, under Grant No. 69-1663-A, and facilities provided by the Advanced Research Projects Agency.

*Advanced Research Projects Agency Predoctoral Fellow.

[1]S. A. Rice, Accounts Chem. Res. 1, 81 (1968).

[2]H. Schnyders, S. A. Rice, and L. Meyer, Phys. Rev. Letters 15, 187 (1965).

[3]H. Schnyders, S. A. Rice, and L. Meyer, Phys. Rev. 150, 127 (1966).

[4]D. W. Swan, Proc. Phys. Soc. (London) 83, 659 (1964).

[5]H. D. Pruett and H. P. Broida, Phys. Rev. 164, 1138 (1967).

[6]L. S. Miller and W. E. Spear, Phys. Letters 24A, 47 (1967).
[7]L. S. Miller, S. Howe, and W. E. Spear, Phys. Rev. 166, 871 (1968).
[8]J. Lekner, Phys. Rev. 158, 130 (1967).
[9]W. A. Schmidt and A. O. Allen, J. Chem. Phys. 52, 4788 (1970).
[10]H. S. Massey and E. H. S. Burhop, *Electronic and Ionic Impact Phenomena* (Oxford U. P., Oxford, England, 1952).
[11]J. Lekner, Phys. Letters 27A, 341 (1968).
[12]J. Lekner, Phil. Mag. 18, 1281 (1968).
[13]B. Halpern and R. Gomer, J. Chem. Phys. 51, 1031 (1969).
[14]L. D. Ikenberry and S. A. Rice, J. Chem. Phys. 39, 1561 (1963).
[15]Obtainable from the Latronics Corp., 901 Lloyd Ave., Latrobe, Pa. 15650.
[16]A. M. Tyndall and C. F. Powell, Proc. Roy. Soc. (London) A129, 162 (1930).
[17]F. Reif and L. Meyer, Phys. Rev. 119, 1164 (1960).
[18]H. T. Davis, S. A. Rice, and L. Meyer, J. Chem. Phys. 37, 2470 (1962).
[19]B. Halpern, J. Lekner, S. A. Rice, and R. Gomer, Phys. Rev. 156, 351 (1967).
[20]A. L. Gosman, Ph. D. thesis, State University of Iowa, 1965 (unpublished), obtainable through University Microfilms, Ann Arbor, Mich.
[21]A. L. Gosman, R. D. McCarty, and J. G. Hurst, National Standard Reference Data Series, Natl. Bur. Std. No. NSRDS-NBS 27 (unpublished).
[22]J. Thoen, E. Vangeel, and W. Van Dael, Physica 45, 339 (1969).
[23]I. S. Radovskii, Zh. Prikl. Mekhan. i Tekhn. Fiz. 3, 172 (1964).
[24]C. Ramsauer and R. Kollath, Ann. Physik 4, 91 (1929).
[25]D. E. Golden and H. W. Bandel, Phys. Rev. 138, A14 (1965).
[26]M. H. Cohen and J. Lekner, Phys. Rev. 158, 305 (1967).
[27]S. Chapman and T. G. Cowling, *The Mathematical Theory of Nonuniform Gases* (Cambridge U. P., New York, 1939). Also, see Ref. 27 for a historical review of the development of this equation.
[28]J. Bardeen and W. Shockley, Phys. Rev. 80, 72 (1950).
[29]N. Kestner and J. Jortner, J. Chem. Phys. (to be published).
[30]P. G. Mikolaj, Ph. D. thesis, California Institute of Technology, Pasadena, Calif., 1965 (unpublished); P. G. Mikolaj and C. J. Pings, J. Chem. Phys. 46, 1401 (1967).
[31]S. C. Smelser, Ph. D. thesis, California Institute of Technology, Pasadena, Calif., 1969 (unpublished).
[32]L. S. Frost and A. V. Phelps, Phys. Rev. 136, A1538 (1964).
[33]D. E. Golden and H. W. Bandel, Phys. Rev. 149, 58 (1965).

PHYSICAL REVIEW A VOLUME 3, NUMBER 2 FEBRUARY 1971

Optical Heterodyne Measurement of Xenon Isotope Shifts

J. Howard Shafer*
Joint Institute for Laboratory Astrophysics, National Bureau of Standards
and
University of Colorado, Boulder, Colorado 80302

Isotope-shift measurements with a precision of two parts in 10^9 of the optical transition frequency were made for the 2.02-μ line of the three even isotopes of xenon: Xe^{132}, Xe^{134}, and Xe^{136}. This shift is extremely small due to the large xenon mass, the proximity of the xenon isotopes to the neutron magic number $N=82$, and the weak interaction of the nucleus with the $5d$ and $6p$ electron states. The measurements were 500 ± 300 kHz ($0.17 \pm 0.01 \times 10^{-3}$ cm^{-1}) for $Xe^{132}-Xe^{134}$ and 1500 ± 300 kHz ($0.050 \pm 0.01 \times 10^{-3}$ cm^{-1}) for $Xe^{134}-Xe^{136}$, where the lighter isotope had the larger transition frequency in each case. These two shifts are sufficiently different to suggest that nuclear field effects contribute to the results.

I. INTRODUCTION

Since optical isotope shifts are very small, better measuring techniques are constantly sought. Recently, lasers have been employed by several groups for such measurements.[1-3] Vetter *et al.*[4-7] have made a systematic study of argon and xenon isotope shifts using a variety of methods involving lasers. The xenon isotopic series falls just before the neutron number 82, and Xe^{136} has this magic number of neutrons. King *et al.*[8] have shown that the total nuclear expansion due to the addition of a neutron decreases rapidly just before $N=82$, and it ought to be extremely small for xenon, so that xenon should exhibit a very small nuclear field effect. Measurements confirm this prediction.[7,9,10]

By far the largest field-effect shifts are due to interactions between the nuclear charge and s or $p_{1/2}$ electron states.[11] For xenon transitions in the infrared, which do not originate or terminate in these levels, the isotope shifts ought to be extremely minute. The transition

$$(^2P^0_{3/2})5d[3/2]^0_1 - (P^0_{3/2})6p[3/2]_1$$